

PAPER • OPEN ACCESS

Towards a high-resolution offshore wind Atlas - The Portuguese Case

To cite this article: A Couto *et al* 2019 *J. Phys.: Conf. Ser.* **1356** 012029

View the [article online](#) for updates and enhancements.



IOP | ebooks™

Bringing you innovative digital publishing with leading voices to create your essential collection of books in STEM research.

Start exploring the [collection](#) - download the first chapter of every title for free.

Towards a high-resolution offshore wind Atlas - The Portuguese Case

A Couto¹, J Silva¹, P Costa¹, D Santos¹, T Simões¹ and A Estanqueiro¹

¹Unidade de Energias Renováveis e Integração de Sistemas de Energia, Laboratório Nacional de Energia e Geologia - LNEG, I.P., Lisboa, Portugal

antonio.couto@lneg.pt, ana.estanqueiro@lneg.pt

Abstract. An accurate offshore wind resource assessment is a key tool for planning marine wind renewable exploitation. To achieve this goal, without resort to an extensive and costly network of anemometric stations or buoys, it becomes necessary to use the so-called atmospheric mesoscale models. This work presents a high spatial resolution (1x1 km) offshore wind resource Atlas for Portugal and the model calibration steps. During the calibration steps, the most adequate: i) atmospheric parameterizations - physics options, ii) initial and boundary conditions (IBC) meteorological datasets, and iii) data assimilation scheme were achieved through sensitivity tests using the common statistical metrics and hourly simulated/observational data. Results show that the most significant improvements are associated with the IBC dataset and the data assimilation scheme used. Thus, the results show that the assimilation procedures coupled with the new ERA-5 reanalysis dataset reduce significantly the errors of the wind speed and direction, especially the normalized mean square error. This reduction, depending on the different calibration setup, can be above 50%. The new Atlas confirms the previous indicators, Portugal presents a high wind power potential, especially for deep offshore regions.

1. Introduction

Offshore wind energy is a key contributor towards the decarbonisation of several electrical power systems. The opportunity for offshore wind deployment worldwide is significant but this technology still presents some technical limitations, especially, for deep offshore regions, and high costs, which includes a reliable wind resource assessment phase [1]. Indeed, an accurate offshore wind resource assessment, the so-called wind Atlas, is a crucial step to establish strategic plans for the marine wind renewable energy exploitation.

The main challenge in evaluating the wind resource consists on installing accurate wind measurement equipment in open sea since a meteorological mast for depths higher than 30 m may not be cost effective [2]. Additionally, open sea wind experimental campaigns are typically collected during a limited spatial and time window, while wind observations inferred through satellites still present large amounts of missing/poor quality data and low spatial/temporal resolution [3]. Thus, to achieve a high quality offshore wind atlas without resort to an extensive and costly network of anemometric stations or buoys, it becomes necessary to use mesoscale numerical models. These models have the ability to describe the atmospheric phenomena for wind power purposes such as the atmospheric turbulence, stratification, land-sea interactions and sea-land-breeze processes.

Several studies have been developed in order to produce regional or national wind atlases being the most popular the European wind Atlas [4]. This study was the first of this kind to produce a wind



(onshore and offshore) atlas for the majority of the European countries. In order to improve the development of wind atlases, several regional studies appeared with more robust mathematical methods to deal with local turbulence phenomena [5–7]. These studies were mathematically focused over specific regional areas such as coastal, forestry areas, complex orography and landscape. It was concluded that the state-of-the-art numerical models used for weather forecast purposes are a valuable tool to produce accurate wind Atlas at regional/national scale. These results are supported by recent works, *e.g.*, [8–11] that computed climatological wind maps for heights near the most common hub height of commercial offshore wind turbines. The results from the previous works were validated using observational data mostly collected from buoys but also inferred from satellites that are capable of describing the wind behaviour only at the sea surface level.

The first offshore wind Atlas for Portugal was produced in 2006 [12]. Thus, taking into account the improvements observed in the numerical simulation field and the lack of measurements to validate the previous Atlas, in this work, a new high spatial resolution wind Atlas is presented based on atmospheric numerical simulations using the MM5 model - "Fifth-generation Mesoscale Model" [13] after optimizing its configuration and input parameters. The optimization relies on identifying the most adequate: i) atmospheric parameterizations - physics options, ii) initial and boundary conditions (IBC) meteorological datasets for model, and iii) meteorological data assimilation scheme. The model is calibrated through sensitive tests using common statistical metrics and the simulated/observational data. The observed meteorological data are collected from different measurements systems, namely, oceanographic buoys, floating Light Detection and Ranging (LiDAR) systems, coastal anemometric masts and horizontal and vertical LiDAR systems using different heights above mean sea level (a.m.s.l.) height. Therefore, the LiDAR datasets available to calibrate the model represent an important contribution of this work since the previous works for assessing the Portuguese offshore wind resource were always validated with measurements collected at near-surface, which neglects some important atmospheric vertical phenomena (*e.g.*, vertical thermal stratification). The high-resolution offshore wind Atlas obtained with this work will allow the identification of adequate areas for offshore wind park deployment supporting the ongoing spatial planning of marine energy sources for the maritime area of Continental Portugal.

Section 2 describes briefly some numerical modelling key features, transversal to every numerical mesoscale model, which can be used to reduce the uncertainty in the wind speed and direction characterization. Section 3 describes the input data and the methodology used. Section 4 presents and discusses the obtained results as well as the new offshore wind Atlas for Portugal. Finally, in section 5 some conclusions are provided.

2. Mesoscale modelling features to improve the wind resource characterization

In the next subsection, a brief background of two relevant mesoscale numerical modelling features addressed in this work is presented. Although some modifications may be necessary, these features can be easily used in all numerical models.

2.1. Meteorological Boundary and Initial Conditions

One of the main sources of error and uncertainty in the wind resource assessment, when numerical mesoscale models are applied, is derived from the initial and boundary conditions (IBC) meteorological data that fed the model, which are essentially atmospheric information provided by reanalysis and/or analysis products [14]. Indeed, several authors show that these data have a crucial impact on the outcomes of the mesoscale model [15–17]. In addition to the physical parameterizations used by each global model that provide IBC meteorological datasets, the key differences between the IBC available are related to the: i) amount of observational data assimilated as well as the type of observational atmospheric equipment's used; ii) data assimilation system; and iii) spatial horizontal and vertical resolution. Based on the aforementioned literature in table 1, a comparison of the different analysis and reanalysis datasets is provided. It should be highlighted that the results in the relevant literature [3,15,16,18,19] show that it is not completely clear which meteorological IBC product is the best since they present quite similar results and often the best product changes from one site to

another. Therefore, a sensitivity test of each IBC product for the region under study is always recommended.

Table 1. Main characteristics of the most commonly applied IBC products (Adapted from: [3]).

Dataset	Time res. (hours)	Assimilation system	Horizontal res. (Lat. X Lon.)	Vertical levels	Temporal coverage
NCEP-R2	6	3D-Var	2.50° x 2.50°	28	1979–Present
CFSR	6	3D-Var	0.50° x 0.50°	64	2011–Present
ERA-I	6	4D-Var	0.75° x 0.75°	60	1979–Present
GFS	6	3D-Var	0.25° x 0.25°	64	2015–Present
FNL	6	3D-Var	1.00° x 1.00°	52	1999–Present
ERA-5	1	4D-Var	0.28° x 0.28°	72	2010–Present

2.2. Data Assimilation

The data assimilation consists of a numerical technique where observed data are combined with a “first guess” or “background forecast” product derived from a numerical weather prediction model (NWP) [20]. The combination of observations and the model give a reliable representation of the “true” state of the atmosphere or the “analysis” at a defined time. Broadly speaking, there are three different types of data assimilation techniques: the three-dimension variational data analysis (3DVAR) [21,22], the four-dimension variational data analysis (4DVAR) [23] and the four-dimensional data assimilation (FDDA) [24–26] concepts. The 3DVAR consists of an iterative minimization procedure able to minimize errors between the local observations and the “first guess” (or “background forecast”) product. The 4DVAR technique is a more complex method but still similar to 3DVAR. The main difference relies on the error minimization methodology. Commonly, the minimization for the 3DVAR case is performed only for one time, while the 4DVAR case uses the concept of a time window period where different observations at different times are available to build a best-fitted minimization error state of the atmosphere.

In fact, not every type of observation can be assimilated by 3DVAR or 4DVAR methods. For instance, the ones available at high frequency rates such as 10min interval [25]. Generally, observations with high frequency time rates are commonly used for wind power studies since they enable to describe the stratification and turbulence effects, which have a crucial impact in the wind resource characterization. Thus, for high rate time resolution observations, another type of data assimilation scheme should be used, namely the observational FDDA technique. The observational FDDA scheme can deal successfully with high frequency observational data for assimilation purposes presenting a low computational cost. Consequently, the observational FDDA technique is a promising technique for using data with high frequency, which can be an important feature to be included in wind resource assessment evaluations. The FDDA scheme basically adjusts the model’s dynamic balance to adapt the mass field variables and thus correct and reduce errors from the mass fields such as the wind speed [25,26]. This adjustment uses the so-called nudging coefficient, G , the time window, T , and influence radius, R , for observation assimilation [25].

3. Data and Methodology

The new wind offshore Atlas for Portugal, presented in this work, is based on atmospheric numerical simulations using the MM5 model. Figure 1a) shows the methodology applied in this work. The first step was the model calibration regarding the: meteorological initial and boundary conditions (IBC) dataset - step *I.A*), atmospheric parameterization (physics options) - step *I.B*), and meteorological data assimilation procedures - step *I.C*). Thus, the model calibration consists in the identification of the most adequate model configuration’ for each step (step *I.A* – *I.C*), figure 1b.

Common statistical metrics (*e.g.*, the normalized mean square error - RMSE, Bias, Pearson correlation, wind roses, etc.) [1,18] were implemented into an in-house toolbox (designated as *Evaluation Toolbox*) and the simultaneous hourly simulated/observational data were used to calibrate the model outputs. The metrics presented in this work intends to quantify the amplitude (related to the systematic tendency of a forecast model to under or overestimate a predetermined parameter) and the

phase errors (related to temporal consistency and the capability to reproduce the temporal variability of a predetermined parameter) of the model. Although, a special focus will be provided to the RMSE and correlation errors since phase errors can denote a severe weakness in the model performance to describe the wind flow variability [27]. As appointed by several authors, such errors cannot be easily removed by using linear corrections as it is usual for amplitude-related errors (*e.g.*, Bias) [27,28]. Thus, a simulation with lower phase errors is preferred rather than a simulation with reduced amplitude errors [27,28]. This option allows the model to be able to simulate meteorological parameters with required physical consistency, *i.e.*, variability over time. Additionally, for wind power generation purposes, the cubic dependence of wind speed requires low error variability otherwise; meaningful errors in the annual energy production can be obtained. To complement the previous statistical parameters, wind roses and the average wind speed binned into twelve directional sectors were also computed and analysed in this work to provide further insights regarding the directional errors.

Due to the high computational effort required for the simulations, two distinct periods (a month representative of the typical summer and winter weather conditions) were used to calibrate the model – *step I*. After the calibration step, the offshore wind Atlas is produced using three consecutive years of data (2015 – 2018) and it is validated based on the available observed dataset – *step II*. For contractual confidentiality reasons it is not possible to show the average wind speed for some observed measurement systems, and, therefore, the focus will be given to the comparison of the common metrics applied in this type of work.

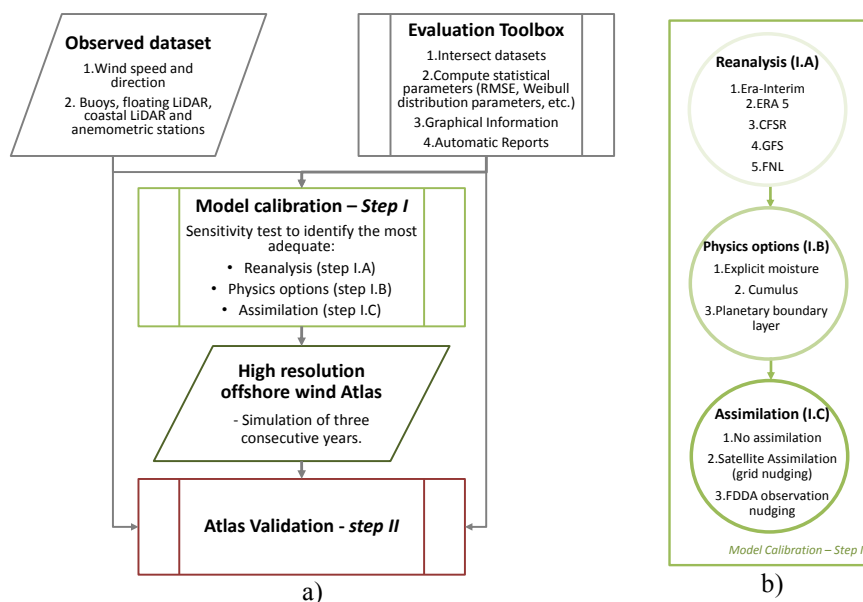


Figure 1. a) A schematic diagram of the methodology applied in this work. b) Different configuration tested in each step of the model calibration – *Step I*.

3.1. Data

3.1.1. Observed dataset. The hourly observed meteorological data are collected from different measurements systems, namely, oceanographic buoys near the Portuguese coast (Raia - RA, Monican01 – M1, Monican02 – M2, Cabo Silleiro – CS and Golf de Cádiz - GC) [29,30], floating (LF) and nacelle (NL) LiDAR systems, coastal anemometric masts (Aguçadoura – AG) and both, horizontal – (Cabo São Vicente – CSV) and vertical (Cabo Penedo Saudade – CPS, Cabo Sardão – Csa) LiDAR systems with different measurement heights a.m.s.l.. The data from buoys are publicly available while the remaining datasets were obtained from national and international projects (*e.g.*, FP7 Norsewind, FP7 DEMOWFLoat and P2020-OFFSHOREPlan). The different measurement systems used during the calibration and validation phase, are depicted in figure 2. The data cover the period from June 2014 to June 2018. The aforementioned data were used only for validation purposes.

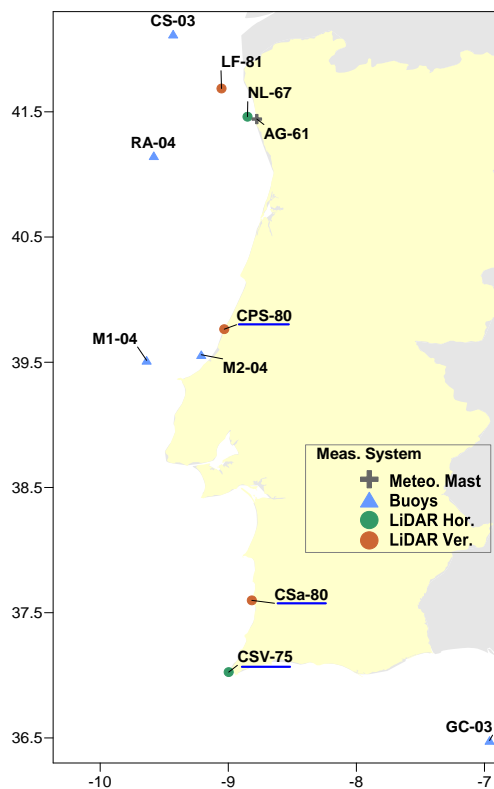


Figure 2. Identification of the measurement systems location, type (symbol) and the measurement height a.m.s.l. used in this work. The underlines represent the data used only during the validation step, while the remaining data were used in both steps (calibration and validation).

3.1.2. Databases used for the different assimilation schemes. Currently, some wind products derived from satellite-observation can provide accurate meteorological data [18] at low levels, typically 10 meters above sea surface level, which can be assimilated in the mesoscale models [31,32]. In this work, the blended mean wind field estimated from scatterometers Advanced SCATterometer (ASCAT) and Oceansat-2 Scatterometer (OSCAT) with a horizontal resolution of 0.25×0.25 degrees and a temporal resolution of 6 hours [33] was employed during the assimilation procedures. Additionally, since the ECMWF reanalysis ERA-5 project [34] presents a spatial (~ 31 km) and temporal (1 hour) resolution it is also adequate for independent data assimilation, and therefore, it was also tested onto the assimilation procedure.

3.2. Mesoscale numerical model and physical parametrizations

Currently, the most applied NWP models in the wind sector are the Weather Research and Forecasting (WRF) and the Mesoscale Fifth Model (MM5) [13,35]. The extensive use of these models can be explained by *i*) their capabilities to accurately describe near surface atmospheric processes and *ii*) the free availability to public use. Despite the physical parameterizations improvement in the WRF mesoscale, the MM5 is still applied by several authors showing a similar and sometimes better performance when compared with WRF model, *e.g.*, [36]. Therefore, and benefiting from the structure developed to generate the first offshore wind atlas for Portugal [12] as well as the previous literature, the MM5 model was selected to obtain the high-resolution (1×1 km) offshore wind atlas.

The orography, vegetation cover and dominant soil type information were obtained from the GTOPO30 [37] and USGS Land Cover database [38] projects, respectively. The numeric simulation was configured *i*) to restart every day during the simulation period and *ii*) for recording data every hour in three domains using a one-way nesting technique with spatial resolutions of 25, 5 and 1 km, figure 3. For all domains, a vertical grid with 26 irregular sigma layers was considered.

The MM5 model allows the selection of several parametrizations to simulate physical processes such as radiation, planetary boundary layer, cloud microphysics, among others. To characterize as accurately as possible the wind speed and direction, the following physical processes, with the greatest impact on the wind resource characterization, were evaluated: explicit moisture schemes - IMPHYS;

planetary boundary layer schemes IBLTYP; and cumulus schemes – ICUPA, table 2. The options tested are in bold in table 2 leading to eighteen different combinations.

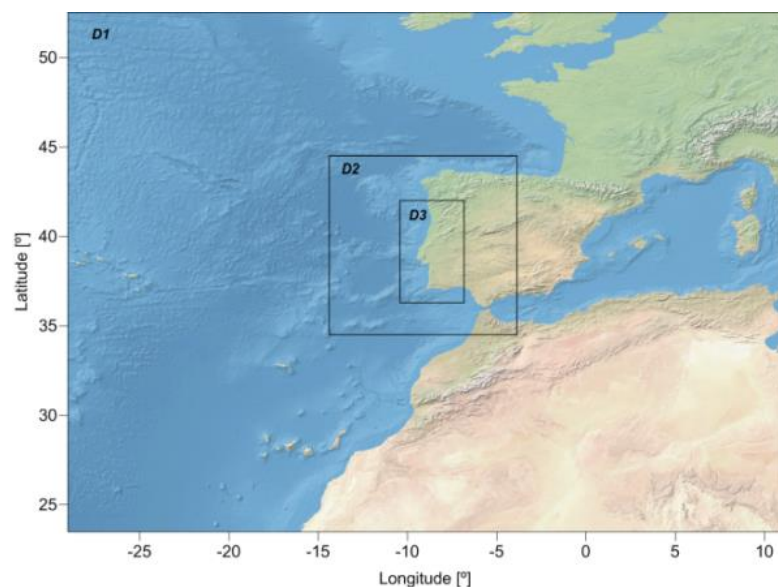


Figure 3. The three nested domains for the MM5 simulation (D1 – 25km; D2 – 5km and D3 – 1 km).

Table 2. Physical options available on the MM5 model.

IMPHYS	IBLTYP	ICUPA
1-Dry	1-none	1-none
2-Stable Precipitation	2- Bulk PBL	2-Anthes-Kuo
3-Warm rain	3-Blackadar	3-Grell
4-Simple ice	4-Burk-Thompson	4-Arakawa-Schubert
5-Mixed-phase	5-Eta	5-Fritsch-Chappell
6-Goddard	6-MRF	6-Kain-Fritsch
-	7-Gayo-Seaman	7-Betts-Miller
-	8-Pleim-Chang	8-Kain-Fritsch 2

4. Results

4.1. Initial and boundary conditions

Taking into account the information from table 1 and works recently published regarding the wind speed assessment [3], five different meteorological IBC were tested (ERA-I, ERA-5, CFSR, GFS and FNL). In table 3, the statistical parameters (correlation, bias and RMSE) of the comparison between observed and simulated wind data by feeding the MM5 model with different meteorological IBC are presented.

Overall, the ERA-5 IBC dataset presents the best performance. For the wind speed, this dataset exhibits the highest correlation and the lowest RMSE values. For all simulations, the wind speed bias values are negative, indicating a tendency, on average, of the model to overestimate the wind speed, when compared with the observed data. For this statistical parameter, the best performance was attained by CFSR product. Regarding the average values of correlation, for the analysed IBC products, a high similarity was observed, nearly, 0.7. Figure 4a shows the average wind speed for the different wind direction sector. Results show that there are no directional systematic errors across the different measurement points, and the model performance is quite similar between the different IBC datasets, as previously discussed.

The average correlation value for wind direction is nearly 0.7. Results show a positive bias in the wind direction, meaning that the model has a tendency to simulate the wind with a slight anti-clockwise

wind rotation. The reduced values of the bias for the different products enable to obtain, on average, a suitable characterization of wind direction, as depicted in figure 4b. According to this figure, with exception of GC station, the prevailing direction sector is only well identified for each measurement point using the ERA-5 IBC dataset.

Table 3. Statistical parameters of the comparison between observed and simulated wind data—step 1.A.

IBC dataset	Correlation		Bias		RMSE	
	Wind Speed [Adim.]	Wind Direction [Adim.]	Wind Speed [m/s]	Wind Direction [°]	Wind Speed [m/s]	Wind Direction [°]
ERA-I	0.70	0.67	-0.32	7.53	2.47	54.10
ERA-5	0.71	0.72	-0.27	6.11	2.34	49.56
CFSR	0.69	0.68	-0.21	8.35	2.51	51.77
GFS	0.71	0.70	-0.27	7.37	2.48	50.21
FNL	0.71	0.68	-0.28	6.83	2.48	50.12

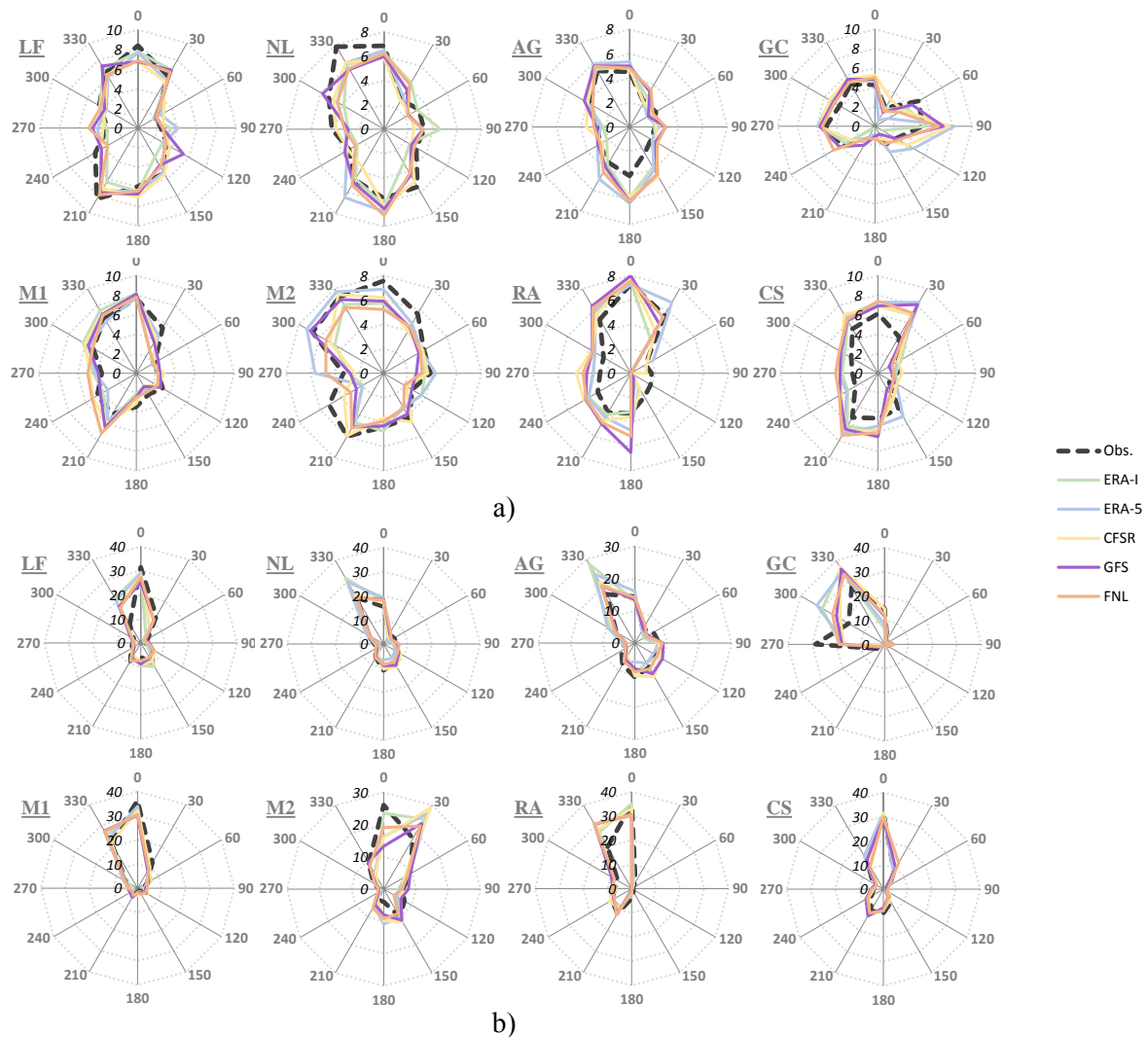


Figure 4. Observed vs. model simulation results according to IBC dataset parameterizations: a) average wind speed for each direction sector and b) wind roses. The two letters at the top represent the name of each measurement location as presented in Figure 2.

4.2. Physical parameterizations

Considering the physical parameterizations indicated in section 3.2, in table 4, the correlation, bias and RMSE values between the measured and simulated wind speed and direction are presented. Figure 5 shows the average wind speed binned by wind direction and the wind rose. In this figure, since only minor differences were observed between each set of physical parameterizations, only two simulations for each set of IMPHYS were selected. The selected simulations are the ones that present lower wind direction RMSE (underlines set of parametrizations in table 4).

Table 4. Statistical parameters of the comparison between observed and simulated wind data—*step I.B.* The underlines represent the physical options that show the lower RMSE within the same IMPHYS set of options.

Physical options (IMPHYS - IBLTYP - ICUPA)	Correlation		Bias		RMSE	
	Wind Speed [Adim.]	Wind Direction [Adim.]	Wind Speed [m/s]	Wind Direction [°]	Wind Speed [m/s]	Wind Direction [°]
2-4-3	0.71	0.72	-0.16	6.25	2.34	49.81
2-4-6	0.70	0.72	-0.18	6.88	2.37	49.72
<u>2-5-3</u>	0.72	0.72	-0.29	6.30	2.30	49.33
<u>2-5-6</u>	0.69	0.72	-0.19	6.94	2.43	49.50
2-7-3	0.71	0.72	-0.27	6.11	2.34	49.56
2-7-6	0.68	0.71	-0.21	6.47	2.45	49.93
<u>4-4-3</u>	0.70	0.71	-0.19	6.81	2.40	50.61
4-4-6	0.68	0.71	-0.14	7.24	2.48	51.18
<u>4-5-3</u>	0.69	0.71	-0.23	6.95	2.43	50.91
4-5-6	0.67	0.70	-0.21	7.13	2.50	50.98
4-7-3	0.69	0.70	-0.24	6.85	2.44	51.47
4-7-6	0.67	0.70	-0.23	6.89	2.49	51.34
5-4-3	0.73	0.72	-0.44	2.14	2.28	50.54
5-4-6	0.72	0.72	-0.46	2.30	2.29	50.52
<u>5-5-3</u>	0.72	0.72	-0.45	1.99	2.32	50.17
<u>5-5-6</u>	0.72	0.72	-0.46	2.01	2.32	50.18
5-7-3	0.72	0.72	-0.49	2.20	2.31	50.51
5-7-6	0.72	0.72	-0.50	2.14	2.32	50.59

From table 4 and figure 5, it is possible to verify a strong similarity in the values between the different parametrization sets. The highest differences are observed for the bias values with IMPHYS equal to 5. Specifically, the wind speed bias is twice the bias identified for the remaining set of parameterization, while for wind direction this set shows the lowest bias values. This set of parameterization tends to show the lowest wind speed RMSE values meaning that it captures better the atmospheric variability. On average, the worst performance was observed for IMPHYS equal to 4 (low correlation and high RMSE values). On the other hand, and taking into account all the statistical parameters the best performance is associated with the set of parameterization IMPHYS equal to 2. Figure 5 supports that only slight differences can be observed between the different set of parameterizations, notwithstanding, the set of parameterization IMPHYS equal to 2 tends to show a higher agreement with the observed values in almost all measurement locations. In this sense, and

although there is no set of physical options that stands out clearly from the others, using the complementary information (*e.g.*, extreme values), it was selected the combination 2-5-3 in this step, which represents a conservative configuration.

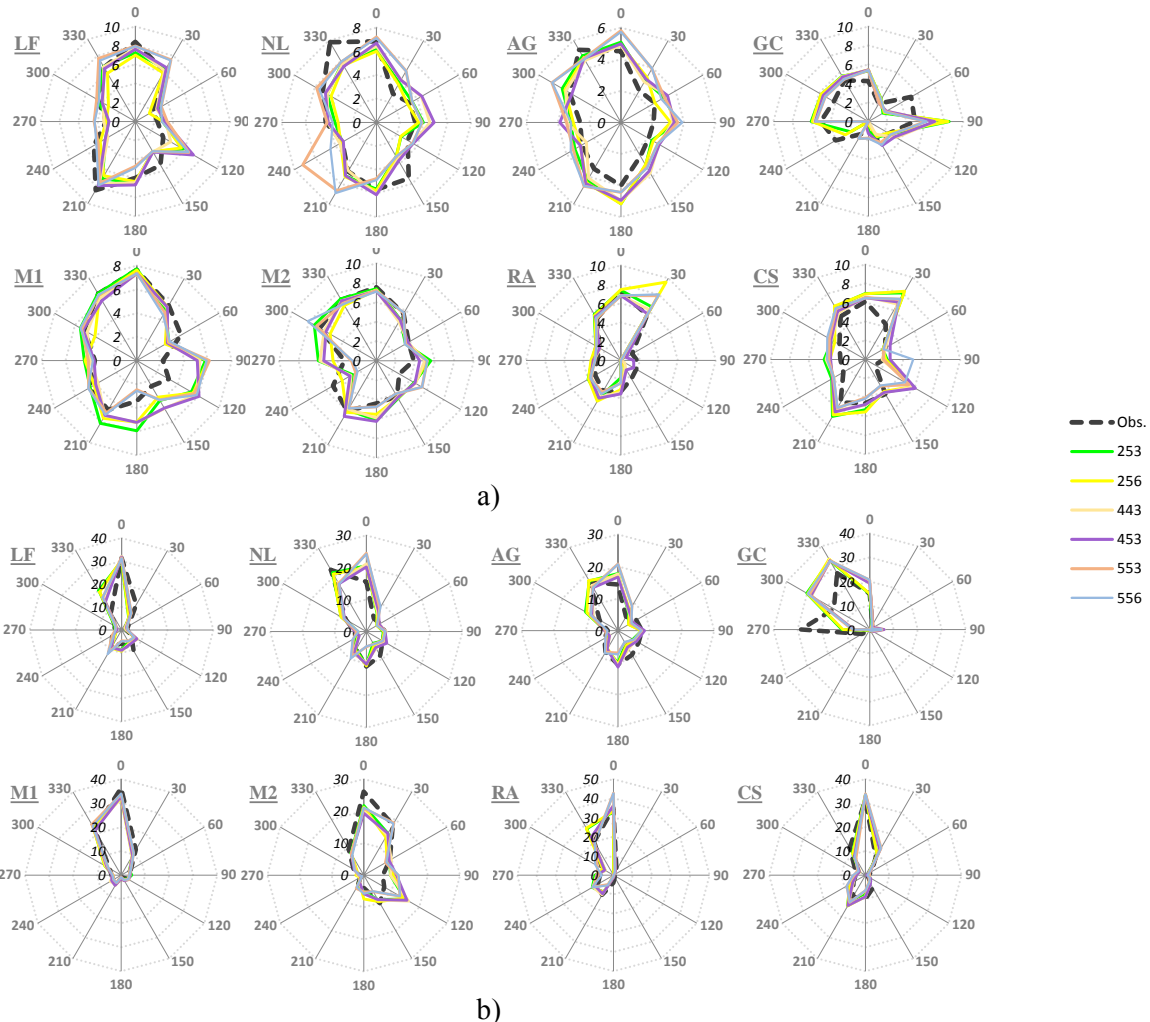


Figure 5. Observed vs. model simulation results according to physical parameterizations: a) average wind speed for each direction sector and b) wind roses. The two letters at the top represent the name of each measurement location as presented in Figure 2.

4.3. Data assimilation

Several sensitivity tests were implemented to identify the most adequate assimilation scheme, the parameters (G, T and R) and the dataset. In table 5, a summary of the best performance achieved using only satellite data assimilation and the scheme FDDA observational technique (hereafter designated as observed-FDDA) using the ERA-5 dataset is presented, while figure 6 shows the average wind speed binned by wind direction and the wind rose.

Table 5 and figure 6 show the benefit of data assimilation for the generation of the wind offshore Atlas for Portugal. A reduced improvement was observed for the assimilation based only on satellite information. This result can be partially explained by the use of information only at a low level of the atmosphere (10 m a.m.s.l.) and with a temporal resolution of 6 hours. On the other hand, meaningful improvements were found with the data assimilation based on information inferred by satellite in the ocean coupled with ECMWF reanalysis ERA-5 project. For wind speed, the observed-FDDA enable to increase 15% the correlation values, and reduce more than 20% the RMSE values when compared with the no assimilation results. Significant benefits are also observed in wind direction characterization. With this assimilation scheme, the wind speed bias error increased twice compared

with the no assimilation results. However, as previously described, linear corrections can be applied to reduce this type of error. Therefore, it was select the observed-FDDA scheme in this step.

Table 5. Statistical parameters of the comparison between observed and simulated wind data- *step I.C.*

Simulation	Correlation		Bias		RMSE	
	Wind Speed [Adim.]	Wind Direction [Adim.]	Wind Speed [m/s]	Wind Direction [°]	Wind Speed [m/s]	Wind Direction [°]
No Assimilation	0.72	0.72	-0.29	6.30	2.30	49.33
Satellite Assimilation (G8,T4,R50)	0.75	0.75	-0.06	5.84	2.15	46.56
Observed-FDDA with ERA-5 (G16,T1,R50)	0.83	0.77	-0.60	2.11	1.78	44.40

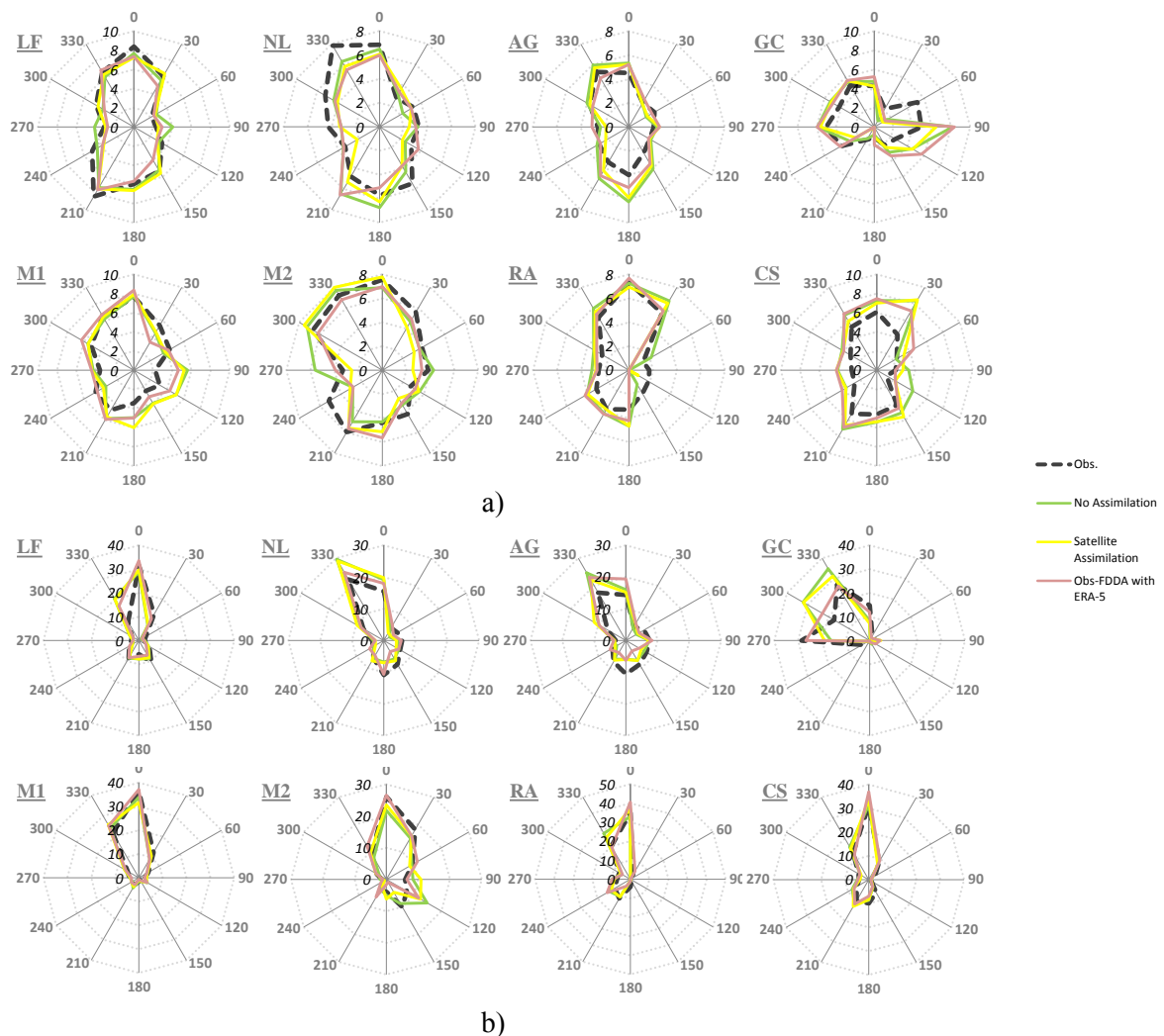


Figure 6. Observed vs. model simulation results without and with different assimilation schemes: a) average wind speed for each direction sector and b) wind roses. The two letters at the top represent the name of each measurement location as presented in figure 2.

4.4. Offshore wind Atlas – Step II

Using the evaluation toolbox and the dataset available during the validation phase, in table 6, the correlation, bias and RMSE values between the measured and simulated wind speed and direction are presented.

Table 6. Statistical parameters of the comparison between observed and simulated wind data- *step II*.

Correlation		Bias		RMSE	
Wind Speed [Adim.]	Wind Direction [Adim.]	Wind Speed [m/s]	Wind Direction [°]	Wind Speed [m/s]	Wind Direction [°]
0.79	0.72	-0.14	8.27	2.55	47.33

For the long-term simulations, and considering all the measurement locations depicted in figure 2, the wind speed presents i) a high correlation value, nearly, 0.80, and ii) a reduced bias error, -0.14 m/s. Comparing with the RMSE obtained during the calibration phase, a slight increase was observed. This result can be partly explained by some extreme weather conditions observed during the three years of simulated data. A systematic overestimation of the wind speed was observed during all simulations (calibration and validation phase), *i.e.*, the wind speed simulated is always slightly above the observed data. For the wind direction, a moderate/high correlation value was achieved, 0.72, while the bias error shows a reduced error. The RMSE for wind direction is in line with the value attained during the calibration phase. Although not shown in detail in this work, the errors observed are not dependent on the measurement height meaning that the vertical stratification of the atmosphere was correctly simulated. In figure 7, the new high-resolution offshore wind Atlas for Portugal is presented.

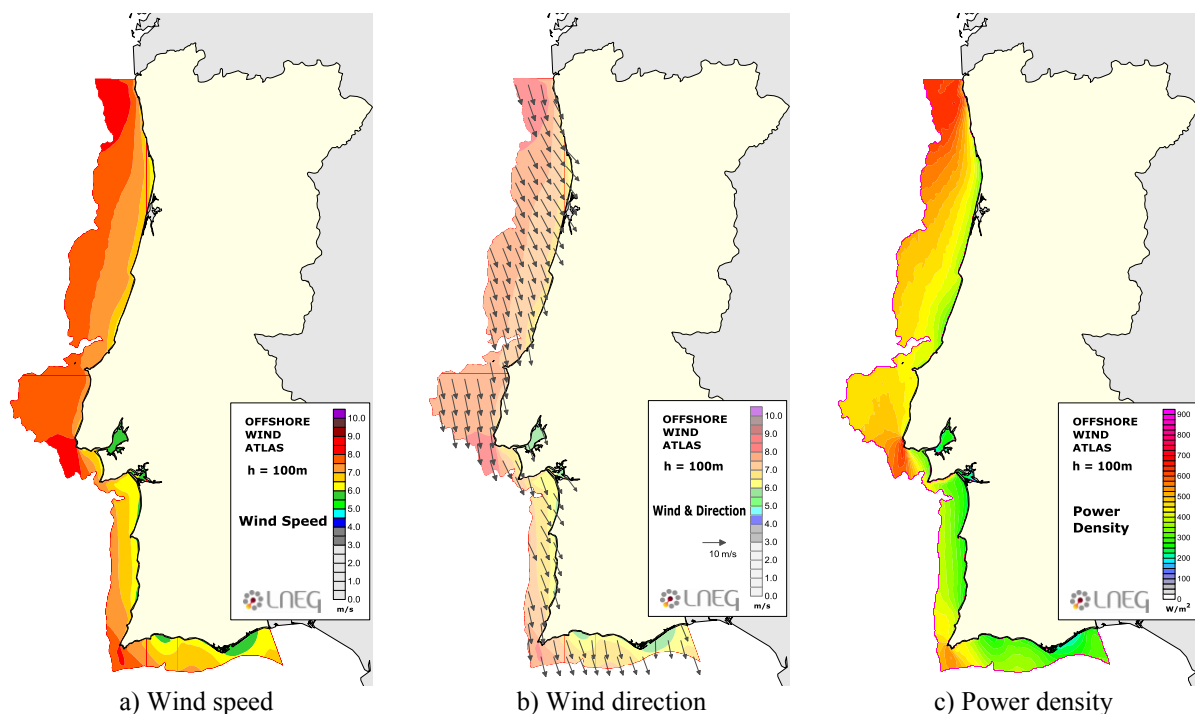


Figure 7. Mean a) wind speed, b) wind direction (computed using the longitudinal and latitudinal wind components) and c) power density values for each cell of the D3 domain (1x1km). Results depicted for 100 meters a.m.s.l..

The results confirm that Portugal has a high wind energy potential, and the northern region is energetically more favourable. Indeed, in this region is foreseen the first Portuguese offshore floating

wind park in 2020. As expected, due to the typical weather conditions observed in Portugal, the most common typical wind directions are from the north/northwest sectors.

5. Conclusions

This paper presents the calibration and model setup procedures for obtaining the new offshore wind Atlas for Portugal with a spatial resolution of 1x1km adequate to describe the atmospheric variability derived from the wind phenomena over the sea and in the cross-border sea/land areas. Given the impracticability of studying, in detail, the Portuguese offshore wind potential using experimental data, the only viable way is through numerical simulations with mesoscale models. To overcome uncertainty associated with the use of these models, a set of sensitivity tests were performed to calibrate the MM5 mesoscale model using observed data gathered in national/international projects (meteorological nearshore meteorological stations, buoys, LiDAR systems). The calibration was focused on the following steps: i) initial and boundary conditions (IBC) meteorological dataset to feed the model, ii) atmospheric parameterization available in the model, and iii) meteorological data assimilation procedures. Using the most adequate calibration for each previous step, the new offshore wind Atlas, based on three years of data, was obtained and validated.

Results show that the calibration procedure is crucial to improve the wind speed and direction characterization. The most meaningful improvement was associated with the data assimilation, followed by the IBC dataset used. On the other hand, the sensitivity tests for the atmospheric parameterization showed small differences among the different options tested. During the calibration phase, the best model setup enabled to obtain: average correlation values of 0.83 and 0.77 for wind speed and direction, respectively, and reduced wind speed RMSE values (1.78 m/s). During the validation phase, the model reduces, slightly, its performance by decreasing the correlation values and increasing the RMSE values. Notwithstanding, a reduction on the bias error to -0.14 m/s was observed.

The validated offshore wind Atlas will support the identification of adequate areas for offshore wind park deployment and allowing to improve the spatial planning of marine energy sources for the maritime area of Continental Portugal. Although further research is required to enable its full validation (*e.g.*, application of linear corrections based on observed data to mitigate the impact of systematic errors), the adoption of assimilation procedures coupled with the state of art of meteorological IBC presents a promising improvement in the accuracy of the wind resource assessment, especially, at regions where observed wind data are not available.

References

- [1] Carvalho D, Rocha A, Gómez-Gesteira M and Santos C S 2014 Offshore wind energy resource simulation forced by different reanalyses: Comparison with observed data in the Iberian Peninsula *Appl. Energy* **134** 57–64
- [2] Estanqueiro A, Couto A, Rodrigues L and Marujo R 2014 Wind resource assessment method for floating deep offshore wind turbines *IET Eng. Technol. Ref.* 7
- [3] Carvalho D, Rocha A, Gómez-Gesteira M and Santos C S 2014 Sensitivity of the WRF model wind simulation and wind energy production estimates to planetary boundary layer parameterizations for onshore and offshore areas in the Iberian Peninsula *Appl. Energy* **135** 234–46
- [4] Troen I and Petersen E L 1989 *European wind atlas* (Roskilde: Risø National Laboratory)
- [5] Mortensen N G 2014 *46200 Planning and Development of Wind Farms: Wind resource assessment using the WAsP software Wind Energy E Report 2014*
- [6] Frank H P, Rathmann O, Mortensen N G, Landberg L and Petersen E L 2001 The numerical wind atlas - The KAMM/WAsP method *Wind Energy New Millenn. Proc.* 661–4
- [7] Tammelin B, Bergström H, Botta G, Douvikas S, Rathmann M and MHyvönen R 2001 Verification on wind energy predictions produced by WAsP and some mesoscale models in European mountains *European Wind Energy Conference and Exhibition (EWEC '01)* (Copenhagen) pp 678–685
- [8] Martín Mederos A C, Medina Padrón J F and Feijóo Lorenzo A E 2011 An offshore wind atlas

- for the Canary Islands *Renew. Sustain. Energy Rev.* **15** 612–20
- [9] Yamaguchi A and Ishihara T 2014 Assessment of offshore wind energy potential using mesoscale model and geographic information system *Renew. Energy* **69** 506–15
- [10] Hahmann A N, Vincent C L, Peña A, Lange J and Hasager C B 2015 Wind climate estimation using WRF model output: Method and model sensitivities over the sea *Int. J. Climatol.* **35** 3422–39
- [11] Waewsak J, Landry M and Gagnon Y 2015 Offshore wind power potential of the Gulf of Thailand *Renew. Energy* **81** 609–26
- [12] Costa P, Miranda P and Estanqueiro A 2006 Development and Validation of the Portuguese Wind Atlas *Proceedings of the European Wind Energy Conference 2006* (Athens, Greece) p 9
- [13] Grell G, Dudhia J and Stauffer D R 1994 *A description of the Fifth-generation Penn State/NCAR Mesoscale Model (MM5)*
- [14] Parker W S 2016 Reanalyses and observations: What's the Difference? *Bull. Am. Meteorol. Soc.* **97** 1565–72
- [15] Alvarez I, Gomez-Gesteira M, DeCastro M and Carvalho D 2014 Comparison of different wind products and buoy wind data with seasonality and interannual climate variability in the southern Bay of Biscay (2000–2009) *Deep Sea Res. Part II Top. Stud. Oceanogr.* **106** 38–48
- [16] Wang A and Zeng X 2012 Evaluation of multireanalysis products with in situ observations over the Tibetan Plateau **117** 1–12
- [17] Soukissian T H and Papadopoulos A 2015 Effects of different wind data sources in offshore wind power assessment *Renew. Energy* **77** 101–14
- [18] Carvalho D, Rocha A, Gómez-Gesteira M and Silva Santos C 2017 Offshore winds and wind energy production estimates derived from ASCAT, OSCAT, numerical weather prediction models and buoys – A comparative study for the Iberian Peninsula Atlantic coast *Renew. Energy* **102** 433–44
- [19] Sharp E, Dodds P, Barrett M and Spataru C 2015 Evaluating the accuracy of CFSR reanalysis hourly wind speed forecasts for the UK , using in situ measurements and geographical information *Renew. Energy* **77** 527–38
- [20] Daley R 1993 *Atmospheric Data Analysis* ed C U Press (Cambridge University Press)
- [21] Barker D M, Huang W, Guo Y-R, Bourgeois A J and Xiao Q N 2004 A Three-Dimensional Variational Data Assimilation System for MM5: Implementation and Initial Results *Mon. Weather Rev.* **132** 897–914
- [22] Barker D, Huang X Y, Liu Z, Aulign T, Zhang X, Rugg S, Ajjaji R, Bourgeois A, Bray J, Chen Y E, Demirtas M, Guo Y R, Henderson T, Huang W, Lin H C, Michalakes J, Rizvi S and Zhang X 2012 The weather research and forecasting model's community variational/ensemble data assimilation system: WRFDA *Bull. Am. Meteorol. Soc.* **93** 831–43
- [23] Huang X-Y, Xiao Q, Barker D M, Zhang X, Michalakes J, Huang W, Henderson T, Bray J, Chen Y, Ma Z, Dudhia J, Guo Y, Zhang X, Won D-J, Lin H-C and Kuo Y-H 2009 Four-Dimensional Variational Data Assimilation for WRF: Formulation and Preliminary Results *Mon. Weather Rev.* **137** 299–314
- [24] Hoke J E and Anthes R A 1976 The Initialization of Numerical Models by a Dynamic-Initialization Technique *Mon. Weather Rev.* **104** 1551–6
- [25] Kuo Y-H and Guo Y-R 1989 Dynamic Initialization Using Observations from a Hypothetical Network of Profilers *Mon. Weather Rev.* **117** 1975–98
- [26] Stauffer D R and Seaman N L 1990 Use of Four-Dimensional Data Assimilation in a Limited-Area Mesoscale Model. Part I: Experiments with Synoptic-Scale Data *Mon. Weather Rev.* **118** 1250–77
- [27] Carvalho D, Rocha A and Gómez-Gesteira M 2012 Ocean surface wind simulation forced by different reanalyses: Comparison with observed data along the Iberian Peninsula coast *Ocean Model.* **56** 31–42
- [28] Lange M and Focken U 2006 *Physical Approach to Short-Term Wind Power Prediction* (Berlin, Heidelberg: Springer)
- [29] Instituto Hidrográfico 2017 *Marinha Portuguesa*

- [30] Puertos del Estado 2017 Ministry of Public Works
- [31] Lorenz T and Barstad I 2013 Wind climatology in the North Sea with WRF **128** 18053
- [32] Peng G, Zhang H-M, Frank H P, Bidlot J-R, Higaki M, Stevens S and Hankins W R 2013 Evaluation of Various Surface Wind Products with OceanSITES Buoy Measurements *Weather Forecast.* **28** 1281–303
- [33] Bentamy A 2016 *Product User Manual for Wind product WIND_GLO_WIND_L4_NRT_OBSERVATIONS_012_004*
- [34] ECMWF 2018 ERA5 data documentation
- [35] Skamarock W C, Klemp J B, Dudhia J, Gill D O, Liu Z, Berner J, Wang W, Powers J G, Duda M G, Barker D M and Huang X-Y 2019 *A Description of the Advanced Research WRF Version 3*
- [36] Salvação N, Bernardino M and Guedes Soares C 2014 Assessing mesoscale wind simulations in different environments *Comput. Geosci.* **71** 28–36
- [37] USGS 2004 Global 30 arc-second topographic database (website)
- [38] USGS 2004 Land Cover Characteristics database (website)

Acknowledgments

This work was supported by the FP7 Norsewind (Grant number: 219048) and DEMOWFloat (Grant number: 296050) projects and, co-financed by the Operational Program for Sustainability and Efficiency in the Use of Resources (POSEUR) through Portugal 2020 and the Cohesion Fund (OffshorePlan Project - POSEUR - 01-1001-FC-000007) and the FCT (Fundação para a Ciência e Tecnologia) through OptiGRID project (PTDC/EEI-EEE/31711/2017).